



Momordicoside G Regulates Macrophage Phenotypes to Stimulate Efficient Repair of Lung Injury and Prevent Urethane-Induced Lung Carcinoma Lesions

Zhenhua Du^{1†}, Shuhui Zhang^{1†}, Yukun Lin¹, Lin Zhou¹, Yuehua Wang¹, Guixi Yan¹, Mengdi Zhang¹, Mengqi Wang¹, Jiahuan Li^{1*}, Qiaozhen Tong^{3*}, Yongjian Duan⁴ and Gangjun Du^{1,2*}

OPEN ACCESS

Edited by:

Annarosa Arcangeli,
University of Florence, Italy

Reviewed by:

Anna Lisa Palange,
Istituto Italiano di Tecnologia, Italy
Agnieszka Zdzisława
Robaszkiewicz,
University of Łódź, Poland

*Correspondence:

Gangjun Du
10200029@vip.henu.edu.cn
Jiahuan Li
jjhuan1020@126.com
Qiaozhen Tong
qztong88@126.com

†These authors have contributed
equally to this work

Specialty section:

This article was submitted to
Pharmacology of Anti-Cancer Drugs,
a section of the journal
Frontiers in Pharmacology

Received: 07 December 2018

Accepted: 15 March 2019

Published: 29 March 2019

Citation:

Du Z, Zhang S, Lin Y, Zhou L,
Wang Y, Yan G, Zhang M, Wang M,
Li J, Tong Q, Duan Y and Du G (2019)
Momordicoside G Regulates
Macrophage Phenotypes to Stimulate
Efficient Repair of Lung Injury
and Prevent Urethane-Induced Lung
Carcinoma Lesions.
Front. Pharmacol. 10:321.
doi: 10.3389/fphar.2019.00321

¹ Institute of Pharmacy, College of Pharmacy, Henan University, Kaifeng, China, ² School of Pharmacy and Chemical Engineering, Zhengzhou University of Industrial Technology, Xinzheng, China, ³ College of Pharmacy, Hunan University of Chinese Medicine, Changsha, China, ⁴ Department of Oncology, The First Affiliated Hospital of Henan University, Kaifeng, China

Momordicoside G is a bioactive component from *Momordica charantia*, this study explores the contributions of macrophages to the effects of momordicoside G on lung injury and carcinoma lesion. *In vitro*, when administered at the dose that has no effect on cell viability in M2-like macrophages, momordicoside G decreased ROS and promoted autophagy and thus induced apoptosis in M1-like macrophages with the morphological changes. In the urethane-induced lung carcinogenic model, prior to lung carcinoma lesions, urethane induced obvious lung injury accompanied by the increased macrophage infiltration. The lung carcinoma lesions were positively correlated with lung tissue injury and macrophage infiltration in alveolar cavities in the control group, these macrophages showed mainly a M1-like (iNOS⁺/CD68⁺) phenotype. ELISA showed that the levels of IL-6 and IL-12 were increased and the levels of IL-10 and TGF-β1 were reduced in the control group. After momordicoside G treatment, lung tissue injury and carcinoma lesions were ameliorated with the decreased M1-like macrophages and the increased M2-like (arginase⁺/CD68⁺) macrophages, whereas macrophage depletion by liposome-encapsulated clodronate (LEC) decreased significantly lung tissue injury and carcinoma lesions and also attenuated the protective efficacy of momordicoside G. The M2 macrophage dependent efficacy of momordicoside G was confirmed in a LPS-induced lung injury model in which epithelial closure was promoted by the transfer of M2-like macrophages and delayed by the transfer of M1-like macrophages. To acquire further insight into the underlying molecular mechanisms by which momordicoside G regulates M1 macrophages, we conduct a comprehensive bioinformatics analysis of momordicoside G relevant targets and pathways involved in M1 macrophage phenotype. This study suggests a function of momordicoside G, whereby it selectively suppresses M1 macrophages to stimulate M2-associated lung injury repair and prevent inflammation-associated lung carcinoma lesions.

Keywords: momordicoside G, macrophage phenotypes, lung injury, carcinoma lesions, injury repair

INTRODUCTION

In spite of revised and aggressive approaches to therapy, the five-year survival rate for advanced stage lung cancer has not improved significantly (Markovic et al., 2008). Carcinogenesis is associated with intrinsic cellular changes and inflammatory factors in the tumor microenvironment (Witz, 2008). Epidemiological and preclinical studies have shown that whole food-derived components are associated with reduced risks of cancers (Stan et al., 2008). Recently, *Momordica charantia* has gained significant attention for its anticancer efficacy and its active components against various cancers (Raina et al., 2016). As an edible fruit and folk drug, *M. charantia* is extremely good for health and has been used traditionally for various therapeutic benefits in China, Southeast Asia and South America (Grover and Yadav, 2004). Research over decades has progressively investigated pharmacological actions of *M. charantia*, and the bioactive compounds isolated from *M. charantia* have shown significant anti-cancer activity in cancer cell lines and xenografted mice by regulation of cancer cell protein network (Farooqi et al., 2018). Chemical analysis shows that momordicoside G is a cucurbitane-type triterpene glycoside in *M. charantia* and such compounds were reported to be able to inhibit breast cancer (Ray et al., 2010), colon cancer (Dia and Krishnan, 2016), brain cancer (Duan et al., 2015) and lung cancer (Wang et al., 2012) *in vitro*. In addition, the extracts of *M. charantia* have shown to reduce DMBA-induced skin papilloma and prevent spontaneous mammary tumorigenesis in mice (Ganguly et al., 2000; Nagasawa et al., 2008). Sur et al. (2018) reported that bitter melon prevented the development of 4-NQO-induced oral squamous cell carcinoma by modulating immune signaling. Yang et al. (2018) found that *M. charantia* extract exerted its anti-inflammatory activity in murine macrophages by reducing the action of TAK1 and affecting the activation of NF- κ B and AP-1. "Cancer is a never cured wound" (Rosowski and Huttenlocher, 2015). In our previous study, wound healing could prevent carcinogenesis (Liu et al., 2015). It has been proved that *M. charantia* can be effectively used to treat diabetic wounds (Hussan et al., 2014; Singh et al., 2017). However, whether these pharmacological actions of *M. charantia* are associated with its active component momordicoside G remains unknown, and a comprehensive study on momordicoside G and its beneficial attributes is also lacking. It is well known that macrophages play a key role in tissue injury repair (Gensel and Zhang, 2015; Wynn and Vannella, 2016). Here, we investigated whether momordicoside G can promote wound healing against carcinogenesis and explored the contributions of macrophages to the effects of momordicoside G on lung injury and carcinoma lesion.

Abbreviations: AO, acridine orange; ANOVA, analysis of variance; BSA, bovine serum albumin; DAPI, diamidino-phenylindole; HRP, horseradish peroxidase; hs-CRP, hypersensitive C-reactive protein; IL-6, interleukin-6; IL-10, interleukin-10; IL-12, interleukin-12; LEC, liposome-encapsulated clodronate; LPS, lipopolysaccharide; MTT, thiazole blue; NLRP3, oligomerization domain-like receptor protein; NO, nitric oxide; ROS, reactive oxygen species; SDS, sodium dodecyl sulfate; TGF- β 1, transforming growth factor- β 1.

MATERIALS AND METHODS

Materials

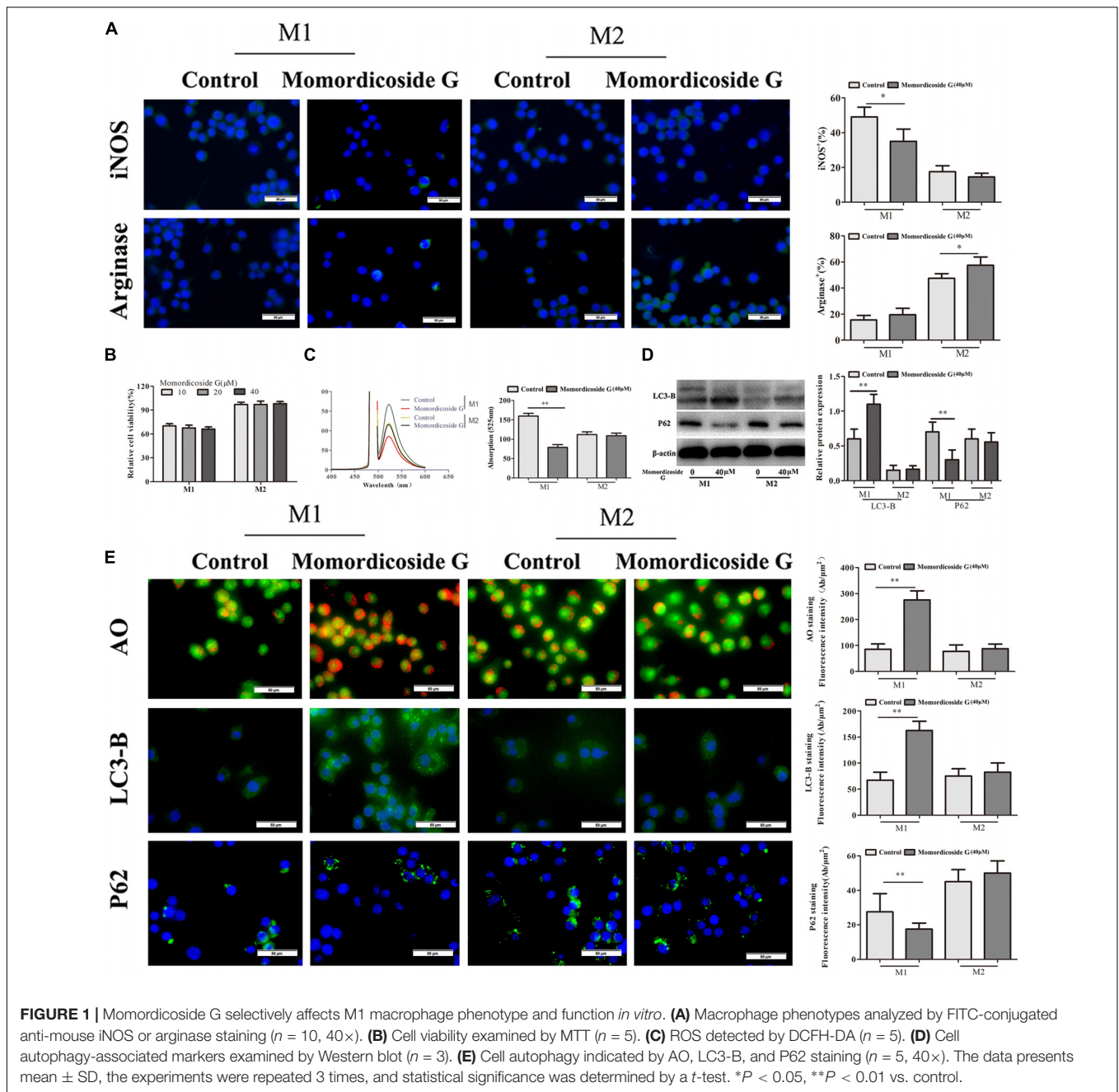
Momordicoside G (purity > 98% via HPLC) from *M. charantia* was purchased from Lianshuo Biotechnology Co., Ltd. (Shanghai, China). RPMI 1640 was obtained from Cellgro (Mediatech, United States). Fetal bovine serum (FBS) was obtained from Hangzhou Sijiqing Biological Engineering Materials Co. (China). Urethane, LPS, DAPI, CFSE, IL-10, AO, and Evans blue were purchased from Sigma Chemical Co. (St. Louis, MO, United States). MTT, DMSO were obtained from Life Technologies (United States). Antibodies used herein including anti-NLRP3, anti-arginase, anti-CD68, anti-iNOS, anti-LC3-B, anti-p62, β -actin, and FITC-conjugated goat anti-mouse IgG were obtained from BD Pharmingen. HRP-conjugated goat anti-mouse IgG polyclonal antibody, Annexin V-FITC Apoptosis kit, ROS, DCFH-DA and mouse quantitative ELISA kits (IL-6, IL-12, IL-10, and TGF- β 1) were obtained from R&D Systems. Nitric oxide (NO) assay kit was obtained from Nanjing Jiancheng Bioengineering Institute. Standard rodent chow was purchased from Henan Provincial Medical Laboratory Animal Center (Zhengzhou, China), License No. SCXK (YU) 2015-0005, Certificate No. 41000100002406.

Animals

Six-week-old female ICR mice were obtained from Henan Provincial Medical Laboratory Animal Center. All mice were housed in individual ventilated cages (lights on 7:00 AM to 7:00 PM). Animals were fed standard rodent chow and water. All animal procedures were approved by the Animal Experimentation Ethics Committee of Henan University (permission number HUSAM 2016-288), and all procedures were performed in strict accordance with the Guide for the Care and Use of Laboratory Animals and the Regulation of Animal Protection Committee to minimize suffering and injury. Animals were euthanized via carbon dioxide overdose based on experimental need.

Cell Culture and Assay

The Raw264.7 macrophages were from ATCC, purchased from the Chinese Academy of Sciences and grown in RPMI 1640 medium supplemented with 10% (v/v) fetal bovine serum (FBS) in a humidified atmosphere containing 5% CO₂ and 95% air at 37°C. Macrophages were seeded in 24-well plates and stimulated by 10 ng/ml LPS or 10 ng/ml IL-10 for 24 h to obtain M1-like (iNOS⁺) and M2-like (arginase⁺) macrophages, subsequently washed once with PBS and cultured in new medium containing different concentrations (10–40 μ M) of momordicoside G for another 24 h. The supernatant was then collected for assays of IL-12, IL-10, TGF- β 1, ROS, and NO. IL-12, IL-10, and TGF- β 1 were tested by ELISA kits, ROS was determined by DCFH-DA, and NO was determined by colorimetric assay kit. The results were calculated from linear curves obtained using the quantikine kit standards. Cell proliferation was examined by MTT reduction assay, according to our previous method (Cao et al., 2016).

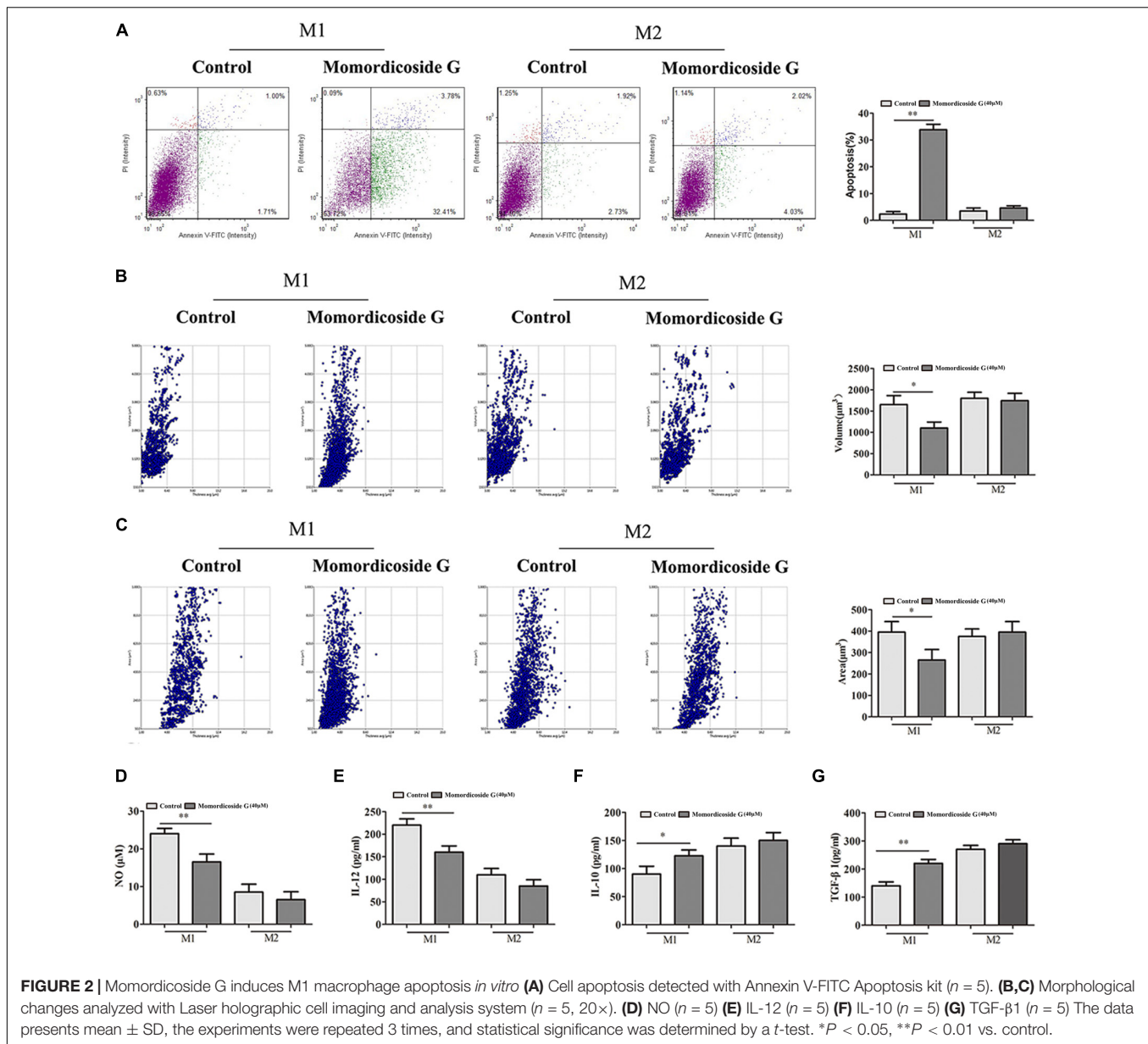


Cells were analyzed by Laser holographic cell imaging and analysis system (HoloMonitor M4, Phiab, Sweden). The immunophenotypes were analyzed by FITC-conjugated anti-mouse-iNOS or anti-mouse-arginase staining. Cells were stained with AO (1 $\mu\text{g/ml}$) at 37°C for 30 min before observation. Red acidic vesicular organelles (AVOs) stained by AO in autophagic cells were visualized under a fluorescence microscope (emission wavelength 488 nm/515 nm). Cell autophagy was further estimated by immunofluorescence staining of LC3-B and p62 production using FITC-conjugated anti-LC3-B or anti-p62. The binding of ANXV-FITC to phosphatidylserine was used as a measure of macrophage apoptosis by an automated

cell counter and analysis system (Nexcelom Cellometer X2, Nexcelom, United States).

Urethane-Induced Lung Carcinogenic Model

Urethane (600 mg/kg body weight) alone or in combined with liposome-encapsulated clodronate (LEC, 4 mg/mouse) was injected intraperitoneally (i. p.) into ICR mice once a week for four or eight weeks (twenty mice per group), according to our previous lung carcinogenic model (Ma et al., 2016). Following the first urethane injection, mice received momordicoside G

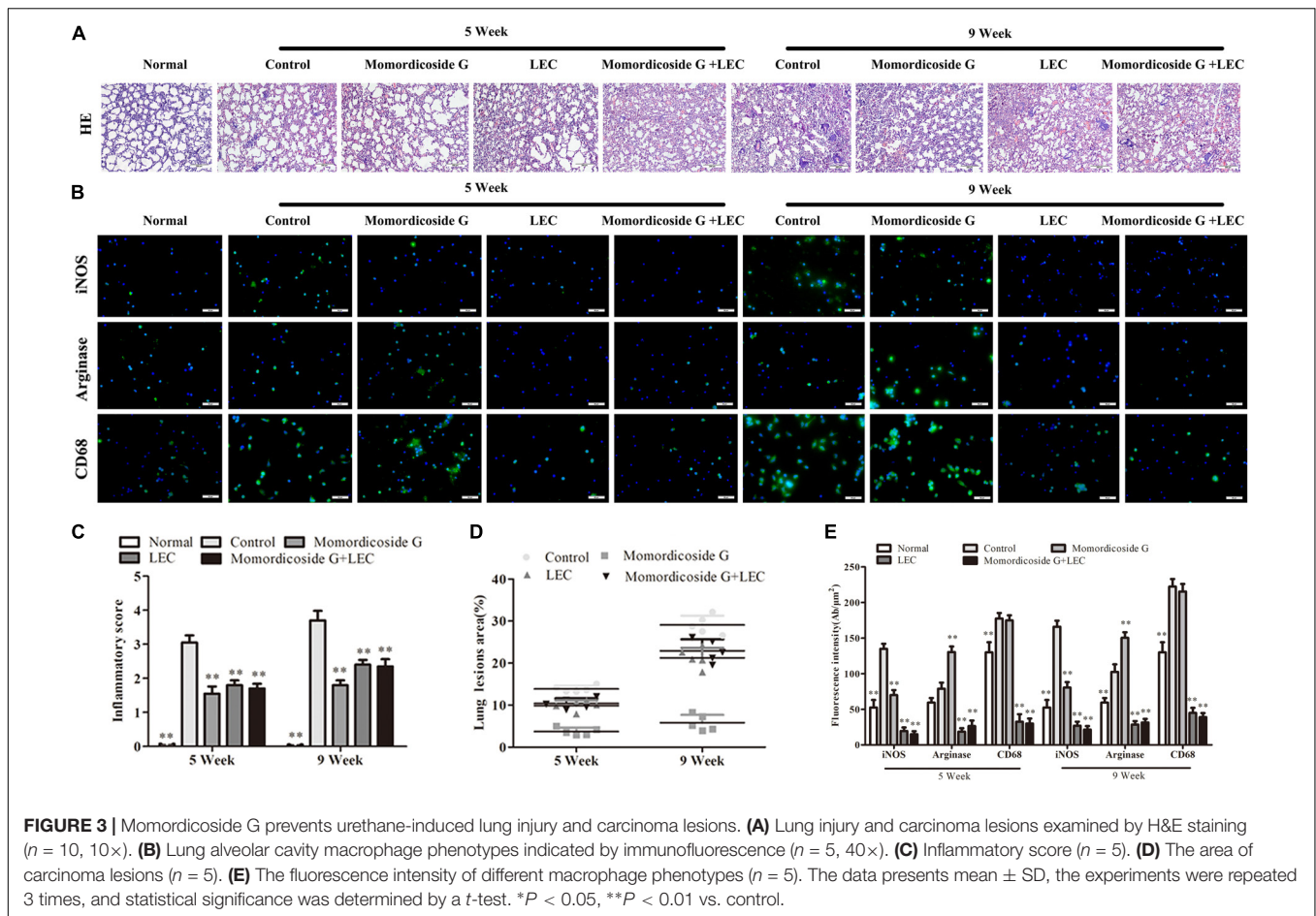


(50 mg/kg/day) once a day via intragastric administration for four or eight weeks. At five and nine weeks after the first urethane injection, ten mice were sacrificed under anesthesia with pentobarbital sodium (90 mg/kg), the alveolar fluid was collected by inserting a cannula into the trachea with three sequential solutions (1 mL PBS), supernatant was used for cytokine assay (IL-6, IL-12, IL-10, and TGF- β 1) after centrifugation, and the centrifuged cells were resuspended in 0.9% sterile saline for total cell counts and added into a magnetic cell sorting column for macrophage collection based on anti-CD68-coated beads.

A part of each lung was preserved in 10% buffered formalin and routinely embedded in paraffin. Lung sections were stained by H&E and immunohistochemistry according to our previously described method (Cao et al., 2016). Inflammatory score (IS) is calculated by the area of involved inflammatory infiltration:

grade 0, no inflammatory infiltration; grades 1, inflammatory infiltration less than 10% of the scanned fields; grade 2, inflammatory infiltration from 10 to 30% of the scanned fields; grade 3, inflammatory infiltration from 30 to 50% of the scanned fields; grade 4, inflammatory infiltration more than 50% of the scanned fields. Atypical adenomatous hyperplasia is regarded as the lung carcinoma lesions based on the histological appearance.

For NLRP3, the total immunohistochemical score was calculated by the intensity score and proportion score by excluding the primary antibody and IgG matched serum, respectively as positive and negative controls. For macrophage phenotypes, after overnight incubation with the primary antibodies (anti-mouse-iNOS, anti-mouse-arginase and anti-mouse-CD68), slides were incubated with the FITC-conjugated goat anti-mouse IgG for 30 min. An automated scanning system



equipped with an Olympus fluorescence microscope was used to determine the positive staining, the total fluorescence intensity was calculated in five successive fields.

Cytokines including IL-6, IL-12, IL-10, and TGF- β 1 were determined.

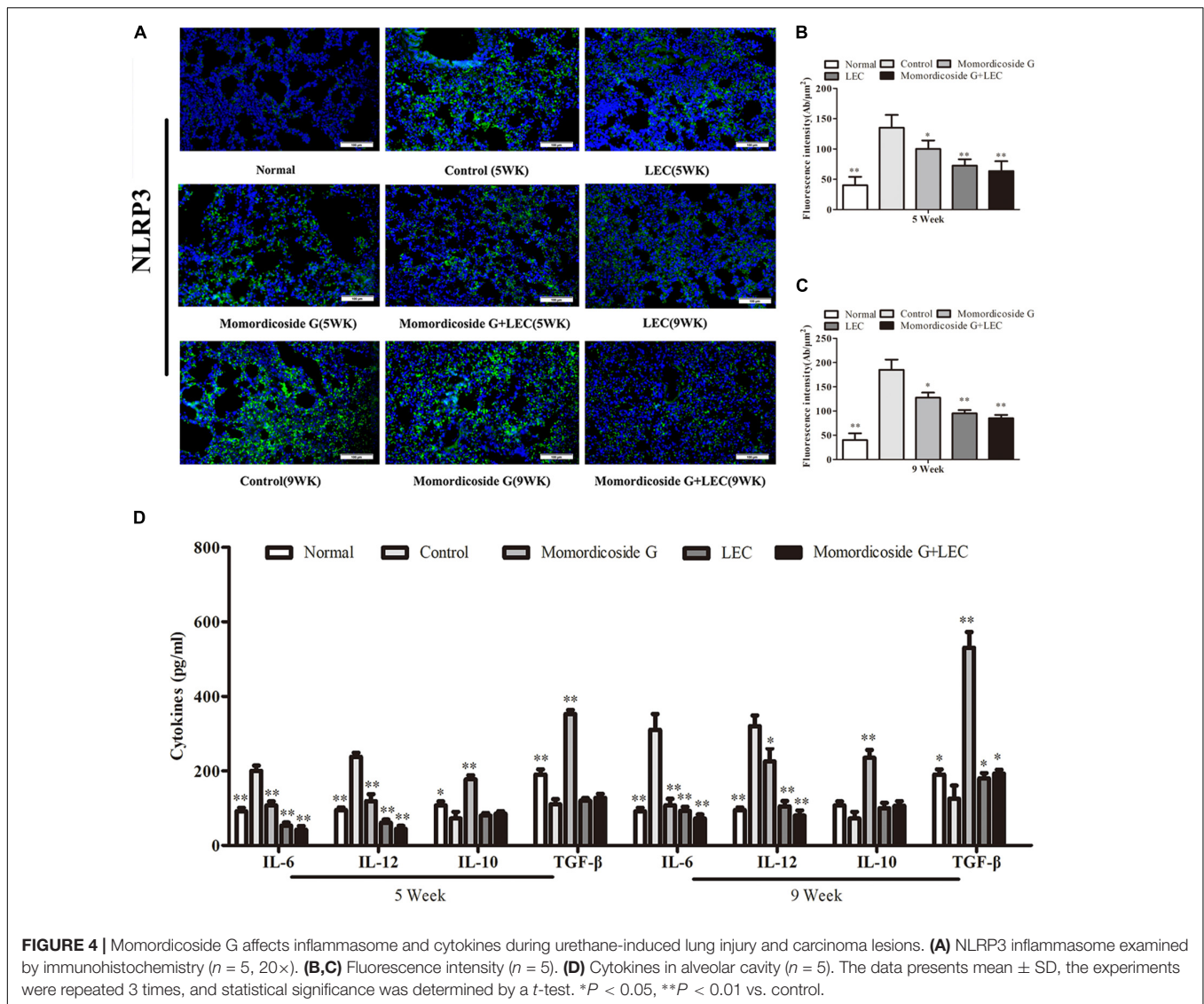
LPS-Induced Lung Injury Model

Lung injury was induced by 2 mg/kg of LPS via intratracheal injection according to previous method (Su et al., 2014) in macrophage-competent and macrophage-deleted mice (twenty mice per group). The macrophage-competent mice only received momordicoside G after LPS injection. For macrophage-depletion, 3 days before lung injury induction, LEC (4 mg/mouse) was injected intraperitoneally into mice. Following LPS injection, *in vitro* IL-10 or LPS-polarized Raw264.7 macrophages (2×10^6 cells in 200 μ L saline) were labeled with CFSE and injected intravenously into mice once a week for two weeks; simultaneously, mice were received momordicoside G (50 mg/kg once a day via intragastric administration) for 2 weeks. Lung function, lung permeability and lung injury were assessed at 2, 8, and 15 days after the lung injury. Lung function was analyzed by maximal mid-expiratory flow using the animal respiratory metabolic measurement system (Sable Systems International, United States). Lung permeability

was assessed with the Evans blue dye extra-barrier technique and the wet/dry ratio of lungs according to our previous method (Meng et al., 2017). Lung injury was evaluated by pathohistological examination. At 15 days, alveolar macrophages were isolated from macrophage-competent mice by magnetic cell sorting based on anti-CD68-coated beads, and lung sections from macrophage-deleted mice were observed under a fluorescence microscope. Protein was extracted from isolated alveolar macrophages in cell lysis buffer. Equal amounts of protein were separated via 12% sodium dodecyl sulfate-polyacrylamide gel electrophoresis (SDS-PAGE), electroblotted on nitrocellulose membranes, and probed with antibodies against iNOS, arginase, LC3-B, and P62. Antibody binding was detected via enhanced chemiluminescence, according to the manufacturer's instructions (Pierce, Rockford, IL, United States). Band density was quantified using ImageJ software (NIH, Bethesda, MD, United States) and normalized to the corresponding control group.

The Regulatory Mechanism of Momordicoside G on Macrophages

The gene expression profiles GSE5099 was obtained from the Gene Expression Omnibus (GEO) database, up- and downregulated genes related to M1-associated macrophages were identified using GEO2R, and the human structures of these



differential proteins were collected from the protein data bank (PDB) for docking. The chemical structure of momordicoside G was obtained from PubChem and the docking exercise was conducted using the online software systems Dock with the auto-removal of non-specified protein structures. Docking scores over 6 was regarded as the potential targets for momordicoside G. The gene ontology (GO) and Kyoto Encyclopedia of Genes and Genomes (KEGG) enrichment analyses were performed for the potential targets using the Database for Annotation, Visualization and Integrated Discovery (DAVID), and the online software OmicsShare. The protein-protein interaction (PPI) among these potential targets was constructed using the STRING database and the hub genes were identified using Cytoscape.

Statistical Analyses

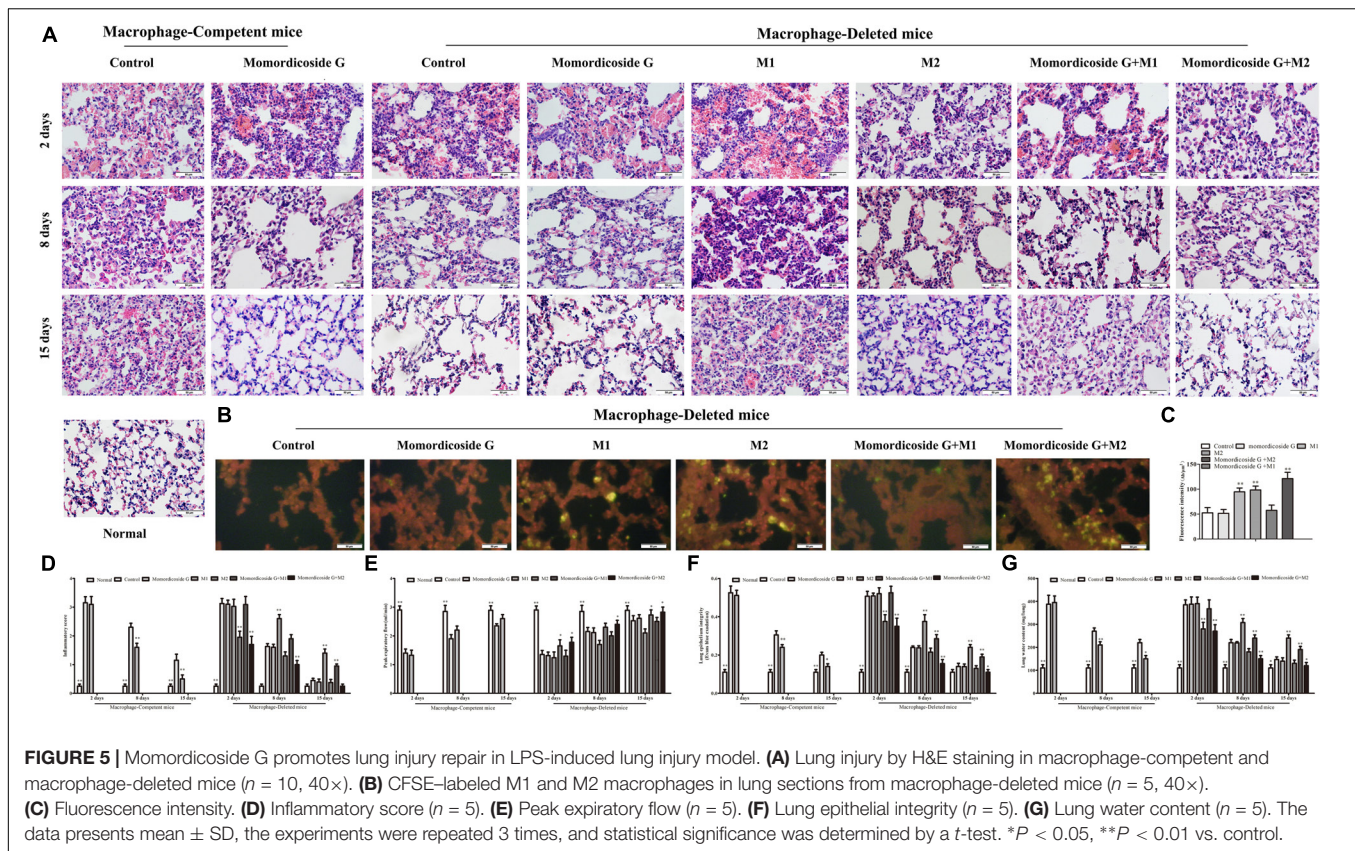
The data was presented as the mean \pm SD and statistically analyzed using GraphPad Prism, Version 5.0 (San Diego, CA, United States). The difference between two groups was

evaluated using a t -test. A P value of less than 0.05 was considered significant.

RESULTS

Momordicoside G Regulates Macrophages *in vitro*

To explore the effects of momordicoside G on macrophages, we stimulated Raw264.7 macrophages with IL-10 to obtain the M2-like cells (arginase⁺ cells) and LPS to obtain the M1-like cells (iNOS⁺ cells) (Figure 1A). Momordicoside G at the dose of 10–40 μ M had no effect on cell viability in M2-like macrophages but suppressed cell proliferation in M1-like macrophages in a dose independent manner (Figure 1B). Further, momordicoside G at the dose of 40 μ M decreased ROS (Figure 1C) and promoted autophagy (Figures 1D,E) and thus induced apoptosis in M1-like macrophages (Figure 2A) with the changes of cell size and



volume (Figures 2B,C). Cytokine assays further proved the effect of momordicoside G on M1-like macrophages, presenting as a decrease in the levels of NO and IL-12 and an increase in the levels of IL-10 and TGF- β 1 (Figures 2D–G).

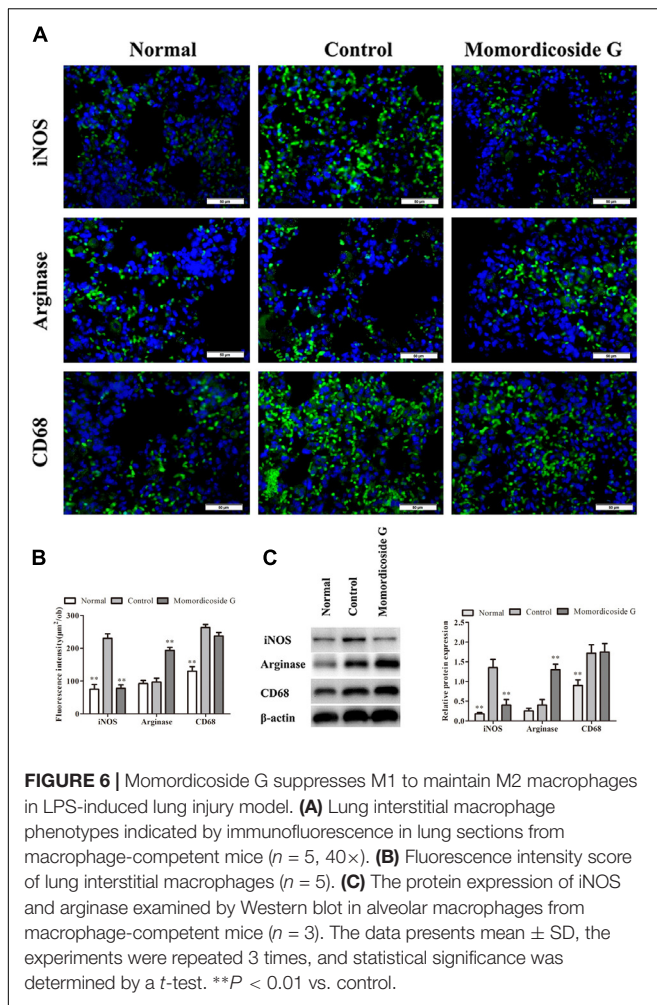
Macrophage Infiltration Play an Important Role in Urethane-Induced Lung Tissue Injury and Carcinoma Lesions

Urethane-induced mouse lung cancer is used for studying basic lung tumor biology and finding new tumor intervention strategies (Du et al., 2013). We found that carcinogenic time can be controlled by the dose and frequency of urethane injection. In this study, urethane at the dose of 600 mg/kg body weight was injected intraperitoneally (i.p.) once a week. At five weeks, prior to lung carcinoma lesions, the four urethane injections led to obvious lung injury in control group (Figure 3A), presenting as an increase in lung inflammation (Figure 3C) and injury area (Figure 3D), which were positively correlated with macrophage infiltration ($CD68^+$ cells) (Figure 3B). Immunohistochemical analysis showed that urethane induced obvious inflammasome, as indicated by staining for nucleotide binding oligomerization domain-like receptor protein 3 (NLRP3) in lung tissues (Figures 4A–C). At nine weeks, the eight urethane injections resulted in visible lung carcinoma lesions (Figure 3A) under a microscope accompanied by the aggravated macrophage

infiltration (Figure 3B) and inflammasome (Figures 4A–C), but no lung cancer nodes were visible to the naked eye. These macrophages had high levels of $iNOS^+/CD68^+$ expression (M1 like) (Figure 3B) and were consistent with the formed inflammasome (Figures 4A–C). ELISA showed that the levels of IL-10 and TGF- β 1 (M2 cytokines) decreased and the levels of IL-6 and IL-12 (M1 cytokines) increased in the alveolar cavity in control mice compared to normal mice (Figure 4D). As expected, macrophage depletion by LEC following urethane injection significantly decreased lung tissue injury and carcinoma lesions (Figures 3A,C) accompanied by a reduction in NLRP3 inflammasome (Figures 4A–C).

Momordicoside G Regulates Macrophages to Prevent Urethane-Induced Lung Injury and Carcinoma Lesions

To prove the preventive effects of momordicoside G on lung injury and carcinoma lesion, mice received momordicoside G after the first urethane injection. At five weeks, compared to the control group, momordicoside G treatment resulted in a reduction in lung injury (Figures 3A,C) accompanied by an increase in M2-like macrophages (arginase $^+$ cells) (Figure 3B) and a decrease in inflammasome (Figures 4A–C) although it had little effect on total macrophages ($CD68^+$ cells) (Figure 3B). At nine weeks, momordicoside G treatment



resulted in not only mild lung tissue injury but also slight carcinoma lesions (Figures 3A,C) which were in line with the decreased M1-like macrophages (iNOS⁺ cells) (Figure 3B) and NLRP3 inflammasome (Figures 4A–C) and the increased levels of alveolar IL-10 and TGF- β 1 (Figure 4D). The effects of momordicoside G on lung injury and carcinoma lesion were significantly attenuated by macrophage depletion (Figures 3, 4).

Momordicoside G Exhibits Macrophage-Regulating Capacity in LPS-Induced Lung Injury Model

To further prove the relativity of momordicoside G-ameliorated lung injury to M2 macrophages, we established an LPS-induced lung injury model in mice with macrophage-depletion or not and used momordicoside G alone or in combination with CFSE-labeled M1-like or M2-like Raw264.7 macrophages to treat the model mice. In macrophage-competent mice, momordicoside G could obviously improve lung injury (Figures 5A,D). In macrophage-deleted mice, the transfer of IL-10-stimulated M2-like macrophages ameliorated lung injury, whereas the transfer of LPS-stimulated M1-like macrophages exacerbated lung injury (Figures 5A,D). Momordicoside G alone did not

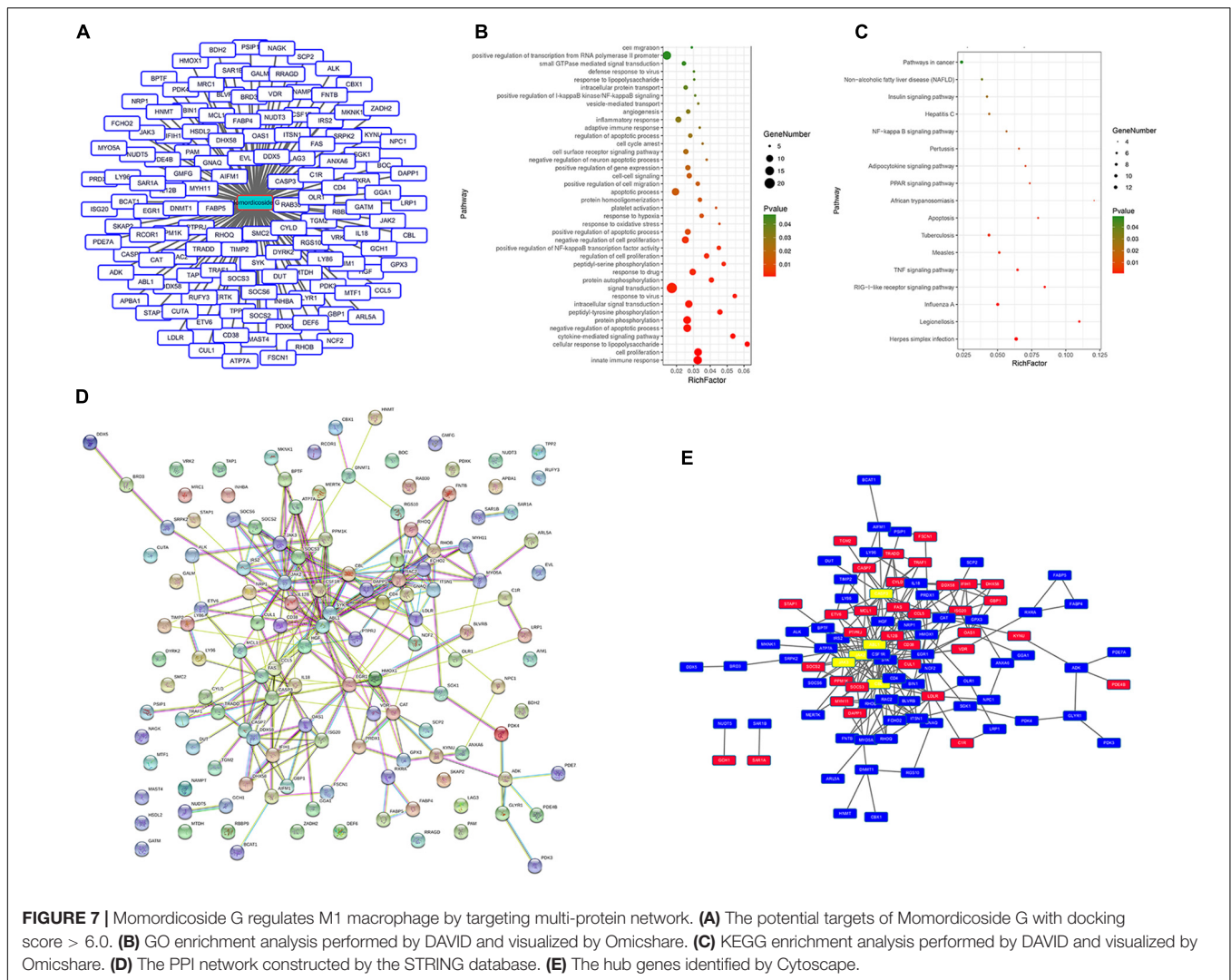
significantly improve lung injury which was aggravated by M1-like macrophages and attenuated by M2-like macrophages (Figures 5A,D). The relativity of ameliorated lung injury to M2 macrophages was further confirmed in lung sections (Figure 5B). However, Momordicoside G decreased the injury-promoting efficacy of M1-like macrophages but synergistically improved lung injury when used in combination with M2-like macrophages accompanied by the improved lung function (Figure 5E) and lung permeability (Figures 5F,G). The M2-like macrophage dependent effect of momordicoside G on lung injury repair was further confirmed in lung sections (Figures 6A,B) in isolated alveolar macrophages by western blot in macrophage-competent mice (Figure 6C).

Momordicoside G Regulates Macrophages by Targeting Multi-Protein Network

We queried 590 up-regulated genes ($\text{LogFC} \geq 1.5$, $P < 0.05$) and 994 down-regulated genes ($\text{LogFC} \leq -1.5$, $P < 0.05$) related to M1-associated macrophages and obtained 181 targeting information. 136 of the potential targets with docking score > 6.0 (pKd/pKi) were selected for GO and KEGG analyses (Supplementary Table S1 and Figure 7A). The hypergeometric distribution count > 4 and $P < 0.05$ were set as threshold criteria to identify the functional gene ontology and pathway. GO enrichment analysis indicated that the potential targets of momordicoside G were primarily associated with the “signal transduction,” “innate immune response,” “cell proliferation,” “protein phosphorylation,” and “apoptotic process” terms (Figure 7B). KEGG enrichment analysis revealed that the potential targets of momordicoside G were significantly enriched in the “Pathways in cancer,” “TNF signaling pathway,” and “RIG-I-like receptor signaling pathway” terms (Figure 7C). The PPI network (Figure 7D) identified 4 key genes (JAK-2, ABL1, CASP3, and CBL), which were hub genes for momordicoside G (Figure 7E).

DISCUSSION

Macrophages are primary phagocytic cells and are also major regulatory cells for tissue homeostasis and injury repair (Lavin et al., 2015). Macrophages can be generally divided into classically activated M1-like macrophages and alternatively activated M2-like macrophages (Mcwhorter et al., 2013). In physiology, lung injury first stimulated M1-like macrophage polarization and later alternatively polarized M2-like macrophages (Sun et al., 2016). It has been reported that the adoptive transfer of M2-like macrophages could accelerate lung repair and reduce lung inflammation as well as lung injury in mice (Tu et al., 2017). In contrast, the depletion of M2-like macrophages exaggerates acute lung injury in mice (Kambara et al., 2015). Consistent with these reports, in this study, urethane-induced lung injury was positively correlated with the number of M1-like macrophages and was negatively correlated with the number of M2-like macrophages, whereas macrophage depletion could significantly decrease lung tissue



injury and carcinoma lesions, indicating an important role of macrophage phenotypes in lung tissue injury and carcinoma lesions. In addition, in this study, momordicoside G treatment resulted in less lung tissue injury and carcinoma lesions accompanied by the decreased M1-like macrophages and the increased M2-like macrophages, whereas macrophage depletion attenuated the protective effect of momordicoside G on lung injury, suggesting a crucial contribution of the retained M2 macrophages to momordicoside G-affected lung injury and carcinoma lesions.

Recently, *M. charantia* consumption increased due to pre-clinical anti-cancer efficacy studies demonstrating bitter melon potential to inducing apoptosis, cell cycle arrest, autophagy and inhibiting cancer stem cells (Dandawate et al., 2016; Gu et al., 2017). Although this plant has high ethnopharmacological value for treating various diseases, anti-inflammatory efficacy should be common mechanisms (Dandawate et al., 2016; Shuo et al., 2017). The injury and cancerization are linked (Tolg et al., 2014). The injury creates a susceptible microenvironment for cancer initiation, and cancerization reflects the aberrant physiological

response to tissue injury (Steiling et al., 2008; Quail and Joyce, 2013). In this study, urethane-induced lung injury was positively correlated with M1-like macrophage infiltration. Considering a cancer-promoting effect of inflammation (Morrison, 2012), we think that M1-like macrophages exert an inflammation-promoting function to prevent injury repair and therefore stimulate carcinoma lesions. Based on the fact that M2-like macrophages exert a protective action on injury, we believe that regulating macrophage phenotypes rather than complete depletion of macrophages is a better approach for injury repair and cancer prevention. In LPS-induced lung injury model, momordicoside G did not improve lung injury in macrophage deleted mice but had synergistical efficacy when used in combination with M2-like macrophages, suggesting a need for M2 macrophage retention. In addition, *in vitro*, momordicoside G decreased ROS and promoted autophagy and thus induced apoptosis in M1-like macrophages but not in M2-like macrophages, indicating a reciprocal inhibition between M1 and M2 cells as well as a selective effect of momordicoside G on macrophage phenotypes. This finding may explain *M. charantia*

consumption against diseases associated with aberrant and uncontrolled inflammation.

Although *M. charantia* and its extracts have been extensively investigated, there is insufficient information related to the mechanism by which *M. charantia* and its extracts exert their anticancer properties in different cancers (Nerurkar and Ray, 2010). It has been proved that *M. charantia* and its extracts can modulate AKT/mTOR/p70S6K signaling, cell cycle regulatory proteins and apoptosis-associated proteins in different cancers (Farooqi et al., 2018). Minari et al. (2018) revealed that there may be possibility of prevention of damage to k-ras gene as a result of the effect of *M. charantia* extract. In this study, we try hard to explain the mechanism by which momordicoside G regulates macrophage phenotypes using bioinformatics analysis and found that the potential targets of momordicoside G regulating macrophages were primarily associated with the “signal transduction,” “innate immune response,” “cell proliferation,” “protein phosphorylation,” and “apoptotic process,” indicating a function of momordicoside G targeting multi-protein network, such as “TNF signaling pathway” and “RIG-I-like receptor signaling pathway,” whereby it regulates macrophage phenotypes to prevent the injury and cancerization. Further mechanism studies are necessary to verify its medicinal applications.

As is the case for other types of cancer, the normal lung cells spend several years transforming into early precursor lesions and finally into lung cancer, which provides us with several opportunities for preventing the progression of precancerous lesions (Gazdar et al., 2011). Although some studies showed a therapeutic effect of *M. charantia* and its compounds on the formatted tumors (Nerurkar and Ray, 2010), we believe that momordicoside G may produce better curative effects as a chemopreventive agent than as a chemotherapeutic agent. Although this study focused on carcinogen-induced mouse lung precancer, based on macrophage regulation, it is likely that momordicoside G and *M. charantia* mediate supplementary benefits for cancer prevention, including reduced chronic inflammation and enhanced injury repair. In addition, momordicoside G as an edible ingredient, logically, its preventive efficacy on lung injury and carcinoma lesions may be overstated in rodent or cell models. With cancer being a global issue and understanding the need for activation of patient’s innate antineoplastic agents, momordicoside G may provide efficient

opportunities as a chemoprevention agent targeting multi-protein network. Certainly, there are visible knowledge gaps related to *M. charantia* and active components in cancer prevention, we need yet develop comprehensive understanding of *M. charantia* and its active components mediated regulation of signal transduction pathways.

In summary, M2-like macrophages play an important role in wound healing and tissue homeostasis, our findings suggest several potential clinical implications. First, there will not be carcinogenesis if tissue injury can be timely and completely cured. Second, Momordicoside G can selectively suppress M1 to maintain M2 macrophages for lung injury repair and therefore prevent inflammation-related lung carcinogenesis. Third, the combination of momordicoside G and M2 macrophages synergistically promote lung injury repair and can be a novel strategy for cancer chemoprevention.

AUTHOR CONTRIBUTIONS

GD conceived and designed the experiments. GD, ZD, SZ, YL, LZ, YW, GY, MZ, and MW performed the experiments. GD, ZD, and SZ analyzed the data. GD, JL, QT, and YD contributed to reagents, materials and analysis tools. GD, ZD, and SZ wrote the manuscript and plotted the results.

FUNDING

This study was supported by the Natural Science Foundation of Henan Province of China (No. 182300410310) and National Natural Science Foundation of China (No. 81472745).

ACKNOWLEDGMENTS

We thank American Journal Experts (AJE) for language editing.

SUPPLEMENTARY MATERIAL

The Supplementary Material for this article can be found online at: <https://www.frontiersin.org/articles/10.3389/fphar.2019.00321/full#supplementary-material>

REFERENCES

- Cao, N., Ma, X., Guo, Z., Zheng, Y., Geng, S., Meng, M., et al. (2016). Oral kanglaite injection (KITI) attenuates the lung cancer-promoting effect of high-fat diet (HFD)-induced obesity. *Oncotarget* 7, 61093–61106. doi: 10.18632/oncotarget.11212
- Dandawate, P. R., Subramaniam, D., Padhye, S. B., and Anant, S. (2016). Bitter melon: a panacea for inflammation and cancer. *Chin. J. Nat. Med.* 14, 81–100. doi: 10.1016/S1875-5364(16)60002-X
- Dia, V. P., and Krishnan, H. B. (2016). BG-4, a novel anticancer peptide from bitter gourd (*Momordica charantia*), promotes apoptosis in human colon cancer cells. *Sci. Rep.* 6:33532. doi: 10.1038/srep33532
- Du, G., Liu, Y., Li, J., Liu, W., Wang, Y., and Li, H. (2013). Hypothermic microenvironment plays a key role in tumor immune subversion. *Int. Immunopharmacol.* 17, 245–253. doi: 10.1016/j.intimp.2013.06.018
- Duan, Z. Z., Zhou, X. L., Li, Y. H., and Zhang, F. (2015). Protection of *Momordica charantia* polysaccharide against intracerebral hemorrhage-induced brain injury through JNK3 signaling pathway. *J. Recept. Signal Transduct. Res.* 35, 523–529. doi: 10.3109/10799893.2014.963871
- Farooqi, A. A., Khalid, S., Tahir, F., Sabitaliyevich, U. Y., Yaylim, I., Attar, R., et al. (2018). Bitter gourd (*Momordica charantia*) as a rich source of bioactive components to combat cancer naturally: are we on the right track to fully unlock its potential as inhibitor of deregulated signaling pathways. *Food Chem. Toxicol.* 119, 98–105. doi: 10.1016/j.fct.2018.05.024

- Ganguly, C., De, S., and Das, S. (2000). Prevention of carcinogen-induced mouse skin papilloma by whole fruit aqueous extract of *Momordica charantia*. *Eur. J. Cancer Prev.* 9, 283–288. doi: 10.1097/00008469-200008000-00009
- Gazdar, A. F., Brambilla, E., Srivastava, S., and Grizzle, W. E. (2011). Preneoplasia of lung cancer. *Cancer Biomark.* 9, 385–396. doi: 10.3233/CBM-2011-0166
- Gensel, J. C., and Zhang, B. (2015). Macrophage activation and its role in repair and pathology after spinal cord injury. *Brain Res.* 1619, 1–11. doi: 10.1016/j.brainres.2014.12.045
- Grover, J. K., and Yadav, S. P. (2004). Pharmacological actions and potential uses of *Momordica charantia*: a review. *J. Ethnopharmacol.* 93, 123–132. doi: 10.1016/j.jep.2004.03.035
- Gu, H., Lin, R., Wang, H., Zhu, X., Hu, Y., and Zheng, F. (2017). Effect of *Momordica charantia* protein on proliferation, apoptosis and the AKT signal transduction pathway in the human endometrial carcinoma Ishikawa H cell line in vitro. *Oncol. Lett.* 13, 3032–3038. doi: 10.3892/ol.2017.5830
- Hussan, F., Teoh, S. L., Muhamad, N., Mazlan, M., and Latiff, A. (2014). *Momordica charantia* ointment accelerates diabetic wound healing and enhances transforming growth factor- β expression. *J. Wound Care* 23, 400, 402, 404–407. doi: 10.12968/jowc.2014.23.8.400
- Kambara, K., Ohashi, W., Tomita, K., Takashina, M., Fujisaka, S., Hayashi, R., et al. (2015). *In vivo* depletion of CD206⁺ M2 macrophages exaggerates lung injury in endotoxemic mice. *Am. J. Pathol.* 185, 162–171. doi: 10.1016/j.ajpath.2014.09.005
- Lavin, Y., Mortha, A., Rahman, A., and Merad, M. (2015). Regulation of macrophage development and function in peripheral tissues. *Nat. Rev. Immunol.* 15, 731–744. doi: 10.1038/nri3920
- Liu, L., Li, H., Guo, Z., Ma, X., Cao, N., Zheng, Y., et al. (2015). The combination of three natural compounds effectively prevented lung carcinogenesis by optimal wound healing. *PLoS One* 10:e0143438. doi: 10.1371/journal.pone.0143438
- Ma, X., Deng, J., Cao, N., Guo, Z., Zheng, Y., Geng, S., et al. (2016). Lasting glycolytic stress governs susceptibility to urethane-induced lung carcinogenesis in vivo and in vitro. *Toxicol. Lett.* 240, 130–139. doi: 10.1016/j.toxlet.2015.10.021
- Markovic, J., Stojic, J., Zunic, S., Ruzdijic, S., and Tanic, N. (2008). Genomic instability in patients with non-small cell lung cancer assessed by the arbitrarily primed polymerase chain reaction. *Cancer Invest.* 26, 262–268. doi: 10.1080/07357900701708385
- Mcwhorter, F. Y., Wang, T., Nguyen, P., Chung, T., and Liu, W. F. (2013). Modulation of macrophage phenotype by cell shape. *Proc. Natl. Acad. Sci. U.S.A.* 110, 17253–17258. doi: 10.1073/pnas.1308887110
- Meng, M., Geng, S., Du, Z., Yao, J., Zheng, Y., Li, Z., et al. (2017). Berberine and cinnamaldehyde together prevent lung carcinogenesis. *Oncotarget* 8, 76385–76397. doi: 10.18632/oncotarget.20059
- Minari, J. B., Okelola, C. A., and Ugochukwu, N. C. (2018). Analysis of kras gene from induced pancreatic cancer rats administered with *Momordica charantia*, and ocimum ba s ilicum, leaf extracts. *J. Tradit. Complement. Med.* 8, 282–288. doi: 10.1016/j.jtcme.2017.04.003
- Morrison, W. B. (2012). Inflammation and cancer: a comparative view. *J. Vet. Intern. Med.* 26, 18–31. doi: 10.1111/j.1939-1676.2011.00836.x
- Nagasawa, H., Watanabe, K., and Inatomi, H. (2008). Effects of bitter melon (*Momordica charantia* L.) or ginger rhizome (zingiber officinale rosc) on spontaneous mammary tumorigenesis in shn mice. *Am. J. Chin. Med.* 30, 195–205. doi: 10.1142/S0192415X02000302
- Nerurkar, P., and Ray, R. B. (2010). Bitter melon: antagonist to cancer. *Pharm. Res.* 27, 1049–1053. doi: 10.1007/s11095-010-0057-2
- Quail, D. F., and Joyce, J. A. (2013). Microenvironmental regulation of tumor progression and metastasis. *Nat. Med.* 19, 1423–1437. doi: 10.1038/nm.3394
- Raina, K., Kumar, D., and Agarwal, R. (2016). Promise of bitter melon (*Momordica charantia*) bioactives in cancer prevention and therapy. *Semin. Cancer Biol.* 4, 116–129. doi: 10.1016/j.semcancer.2016.07.002
- Ray, R. B., Raychoudhuri, A., Steele, R., and Nerurkar, P. (2010). Bitter melon (*Momordica charantia*) extract inhibits breast cancer cell proliferation by modulating cell cycle regulatory genes and promotes apoptosis. *Cancer Res.* 70, 1925–1931. doi: 10.1158/0008-5472.CAN-09-3438
- Rosowski, E. E., and Huttenlocher, A. (2015). Neutrophils, wounds, and cancer progression. *Dev. Cell* 34, 134–136. doi: 10.1016/j.devcel.2015.07.005
- Shuo, J., Mingyue, S., Fan, Z., and Jianhua, X. (2017). Recent advances in *Momordica charantia*: functional components and biological activities. *Int. J. Mol. Sci.* 18:E2555. doi: 10.3390/ijms18122555
- Singh, R., Garcia-Gomez, I., Gudehithlu, K. P., and Singh, A. K. (2017). Bitter melon extract promotes granulation tissue growth and angiogenesis in the diabetic wound. *Adv. Skin Wound Care* 30, 16–26. doi: 10.1097/01.ASW.0000504758.86737.76
- Stan, S. D., Kar, S., Stoner, G. D., and Singh, S. V. (2008). Bioactive food components and cancer risk reduction. *J. Cell Biochem.* 104, 339–356. doi: 10.1002/jcb.21623
- Steiling, K., Ryan, J., Brody, J. S., and Spira, A. (2008). The field of tissue injury in the lung and airway. *Cancer Prev. Res.* 1, 396–403. doi: 10.1158/1940-6207.CAPR-08-0174
- Su, Z. Q., Mo, Z. Z., Liao, J. B., Feng, X. X., Liang, Y. Z., Zhang, X., et al. (2014). Usnic acid protects LPS-induced acute lung injury in mice through attenuating inflammatory responses and oxidative stress. *Int. Immunopharmacol.* 22, 371–378. doi: 10.1016/j.intimp.2014.06.043
- Sun, K., He, S., Qu, J., Dang, S., Chen, J., Gong, A., et al. (2016). IRF5 regulates lung macrophages M2 polarization during severe acute pancreatitis in vitro. *World J. Gastroenterol.* 22, 9368–9377. doi: 10.3748/wjg.v22.i42.9368
- Sur, S., Steele, R., Aurora, R., Varvares, M., Schwetye, K. E., and Ray, R. B. (2018). Bitter melon prevents the development of 4-nqo-induced oral squamous cell carcinoma in an immunocompetent mouse model by modulating immune signaling. *Cancer Prev. Res.* 11, 191–202. doi: 10.1158/1940-6207.CAPR-17-0237
- Tolg, C., Mccarthy, J. B., Yazdani, A., and Turley, E. A. (2014). Hyaluronan and rhamm in wound repair and the "cancerization" of stromal tissues. *Biomed Res. Int.* 2014:103923. doi: 10.1155/2014/103923
- Tu, G., Shi, Y., Zheng, Y., Ju, M., He, H., Ma, G., et al. (2017). Glucocorticoid attenuates acute lung injury through induction of type 2 macrophage. *J. Transl. Med.* 15:181. doi: 10.1186/s12967-017-1284-7
- Wang, X., Sun, W., Cao, J., Qu, H., Bi, X., and Zhao, Y. (2012). Structures of new triterpenoids and cytotoxicity activities of the isolated major compounds from the fruit of *Momordica charantia* L. *J. Agric. Food Chem.* 60, 3927–3933. doi: 10.1021/jf204208y
- Witz, I. P. (2008). Tumor-microenvironment interactions: dangerous liaisons. *Adv. Cancer Res.* 100, 203–229. doi: 10.1016/S0065-230X(08)00007-9
- Wynn, T. A., and Vannella, K. M. (2016). Macrophages in tissue repair, regeneration, and fibrosis. *Immunity* 44, 450–462. doi: 10.1016/j.immuni.2016.02.005
- Yang, W. S., Yang, E., Kim, M. J., Jeong, D., Yoon, D. H., Sung, G. H., et al. (2018). *Momordica charantia* inhibits inflammatory responses in murine macrophages via suppression of TAK1. *Am. J. Chin. Med.* 46, 435–452. doi: 10.1142/S0192415X18500222

Conflict of Interest Statement: The authors declare that the research was conducted in the absence of any commercial or financial relationships that could be construed as a potential conflict of interest.

Copyright © 2019 Du, Zhang, Lin, Zhou, Wang, Yan, Zhang, Wang, Li, Tong, Duan and Du. This is an open-access article distributed under the terms of the Creative Commons Attribution License (CC BY). The use, distribution or reproduction in other forums is permitted, provided the original author(s) and the copyright owner(s) are credited and that the original publication in this journal is cited, in accordance with accepted academic practice. No use, distribution or reproduction is permitted which does not comply with these terms.